



## EFFECT OF RADIAL FLOW 2-BLADE FLAT TURBINE ON IONIC MASS TRANSFER IN AN ELECTROLYTIC CELL

G. ESTHERU, G. SHRIKANTH, N. CHITTI BABU\*, D. SUBBA RAO and  
P. VENKATESWARLU

Department of Chemical Engineering, Andhra University, VISAKHAPATNAM – 530003 (A.P.) INDIA

(Received : 13.08.2012; Accepted : 22.08.2012)

### ABSTRACT

Limiting current data are obtained using diffusion-controlled cathodic reduction of ferricyanide ion at the microelectrodes fixed on the electrode support and cell wall in an electrolytic cell in the presence of a rotating radial flow 2-blade flat turbine. The mass transfer coefficient is increased with increases in rotational speed, diameter of the turbine, width of the turbine blade and flow rate of the electrolyte.

**Key words:** Limiting current, Electrolytic cell, Turbine, Augmentation technique.

### INTRODUCTION

Different augmentation techniques have been used for improving the ionic mass transfer rates in electrolytic cells. Impellers are one of the important techniques employed for augmenting the mass transfer rates<sup>1-4</sup>. Sedahmed et al.,<sup>1</sup> obtained mass transfer data rotating various turbines in a cylindrical vessel. They proposed the following correlations:

$$Sh_L = 1.727 Sc^{0.33} Re^{0.5} \quad 3,350 < Re < 33,500 \quad \text{for four blade flat turbine}$$

$$Sh_L = Sc^{0.33} Re^{0.6} \quad 3,000 < Re < 60,000 \quad \text{for four blade } 45^\circ \text{ pitched turbine}$$

$$Sh_L = 0.22 Sc^{0.33} Re^{0.75} \quad 3,350 < Re < 37,600 \quad \text{for six blade disc turbine}$$

The better performance was achieved by rotating concave-blade and comb-blade impellers than the standard Rushton impellers and pitched-blade impellers<sup>2</sup>. Lu et al.,<sup>3</sup> reported higher mass transfer coefficients with the quadruple stage system than the triple stage system.

Moucha et al.,<sup>4</sup> correlated the mass transfer coefficient data in a cylindrical vessel for various impeller configurations. Krishna et al.,<sup>5</sup> determined the mass transfer rates at rotating copper cylindrical electrodes in the centre of a baffled vessel and correlated their data as:  $Sh_c/Sc^{1/3} = 1.83 Re_c^{0.58}$ . Bharathi et al.,<sup>6</sup> studied the individual and synergetic effects of vibration and rotation of spheres on mass transfer in an open electrolytic cell. The limiting current data increased with increases in frequency, amplitude and rotational speed. The mass transfer data were correlated as follows.

$$\text{Sh}_v / \text{Sc}^{1/3} = 0.97 \text{Re}_v^{0.49} \quad \text{for vibration}$$

$$\text{Sh}_L / \text{Sc}^{1/3} = 0.97 \text{Re}_r^{0.68} \quad \text{for rotation}$$

$$\text{Sh}_{v,r} / \text{Sc}^{1/3} = 0.052 (\text{Re}_v \text{Re}_r)^{0.4} \quad \text{for simultaneous rotation and vibration}$$

Coeuret and Legrand<sup>7</sup> observed that the local mass transfer coefficient was increased when the annular Reynolds number was increased above 300 on the surface of a rotating inner cylindrical electrode. Afshar et al.,<sup>8</sup> correlated the mass transfer data in turbulent flow for upright rotating cone electrode as  $\text{Sh}_L = 0.04 \text{Re}^{0.95}$ . For inverted rotating cones, the mass transfer data in turbulent flow were presented as  $\text{Sh}_L = 0.04 \text{Re}^{0.88}$ . The mass transfer coefficients were improved by 38 to 600 percent on a disc rotating in a submerged impinging jet in a closed cell<sup>9</sup>. The mass transfer coefficient was decreased with increase in distance between the nozzle and rotating disc surface. Subramaniyan et al.,<sup>10</sup> studied mass transfer rates at spheres, discs and downward facing cones of different sizes rotating about their axis of symmetry in a closed electrolytic cell by employing diffusion-controlled electrode reaction. The mass transfer coefficients increased with rotation of the discs, spheres and cones having apex angles greater than 40°. The data were correlated by the following equations:

$$(k_{Lr}/k_{Lo}) = 0.169 (\omega \sin \alpha / \nu)^{0.5} \quad \text{for cones}$$

$$(k_{Lr}/k_{Lo}) = 0.169 (\omega / \nu)^{0.5} \quad \text{for discs and spheres}$$

Elsner et al.,<sup>11</sup> investigated ionic mass transfer on rotating disc electrode with a hanging electrolyte column. The ionic mass transfer depended on its height above the electrolyte surface. The copper deposition was accelerated up to two fold by increasing the disc electrode rotation rate<sup>12</sup>. Even a slow movement of plating solution raised the copper deposition rate up to 10-fold compared to the stationary solution. Gabe and Mekanjuola<sup>13</sup> studied the effect of roughened rotating cylindrical electrode on mass transfer. The mass transfer rate was increased by 100-300% for turbulent flow in the Reynolds number range of 7000 and 80000. Pokryvailo et al.,<sup>14</sup> studied unsteady mass transfer in turbulent flow close to a rotating cylinder by using potassium ferri-ferrocyanide system. The data were correlated as:  $\text{Sh}_L / \text{Sc}^{0.25} = 0.051 \text{Re}_1^{0.8}$ . Morrison et al.,<sup>15</sup> studied the mass transfer and kinetic characteristics using a platinum rotating cylinder electrode for ferri/ferro redox reaction. They proposed the equation:  $J_{dr} = 0.0964 (\rho \nu_r d / \mu)^{-0.3}$ . Grau and Bisang<sup>16</sup> studied mass transfer at a rotating 35 mm diameter cylinder electrode of woven-wire meshes for the reduction of ferri-cyanide in an undivided batch reactor. The mass-transfer coefficients for rotating cylinder electrode were approximately three times higher than those obtained with smooth electrodes. The data were correlated by the equation:  $\text{Sh}_d / \text{Sc}^{1/3} = 0.967 (\text{Re}_d \times r_2 / \bar{r})^{0.58} (H / \bar{r})^{0.47}$ . Based on the literature survey, the present investigation is undertaken to obtain the mass transfer data on electrode support and cell wall in an open electrolytic cell in the presence of rotating radial flow 2-blade flat turbine. Though the mass transfer equations obtained in this case can not be extended to other types of turbines, this experimentation gives insight into the effectiveness of the 2-blade flat turbine in enhancing mass transfer coefficients in electrolytic cells.

## EXPERIMENTAL

The experimental set up comprises of a storage tank, a 0.5 W centrifugal pump, two rotameters, an electrolytic cell, a 2-blade flat turbine and a 0.25 W motor. The 120 L capacity cylindrical PVC storage tank is connected to the rotameters through the centrifugal pump using a 0.018 m diameter copper pipe. A bypass line with a control valve is provided for the pump to control the flow rate. The rotameters are provided with valves to regulate the flow rate of the electrolyte. The rotameter is connected to the rectangular open electrolytic cell (Fig. 1). The electrolytic cell contains an electrode support (C) and a copper anode (A). The electrode support is a perspex sheet with microelectrodes fixed flush with its surface as shown in Fig. 2.

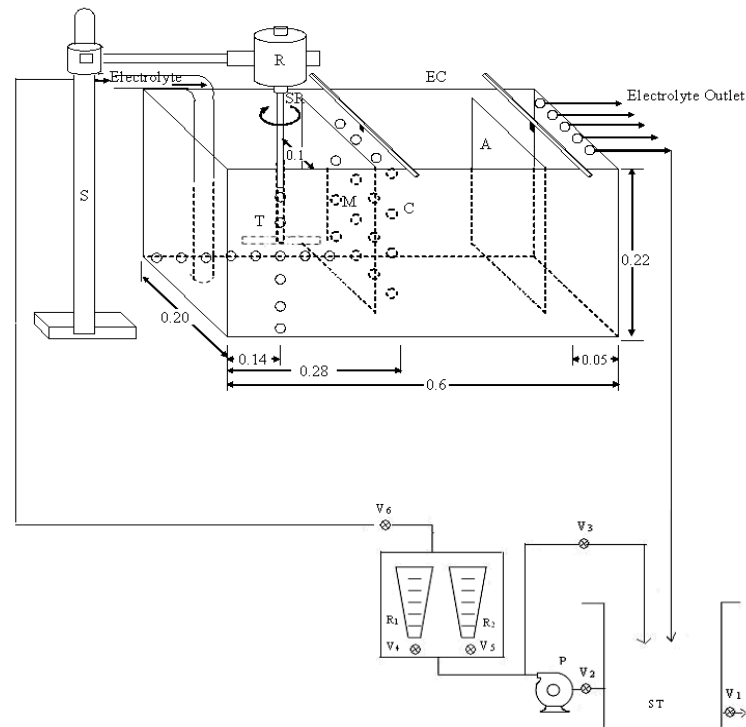


**Fig. 1: Schematic diagram of the experimental set – up (all dimensions in meters)**

EC – Electrolytic cell, P – Centrifugal pump, R – Motor, R<sub>1</sub>, R<sub>2</sub> – Rotameter, ST – Storage tank, T – 2-blade flat turbine, V<sub>1</sub> to V<sub>6</sub> – Control valves.

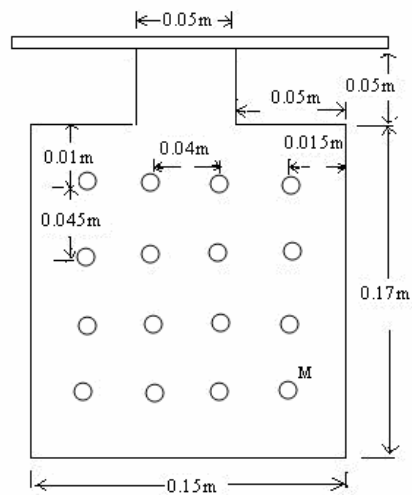


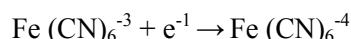
**Fig. 2: Details of the electrode support**

M-Microelectrode

The electrical wires are soldered to the microelectrodes and drawn out through the grooves cut behind the electrode support and connected to a selector switch to facilitate the measurement of limiting current at any desired microelectrode. The electrode support is fixed vertically and firmly in the cell at a distance of 0.28 m from the cell wall (width side) and is situated at 0.035 m height from the cell bottom. The copper anode (A) is also fixed firmly at a distance of 0.05 m from the other cell wall. The microelectrodes are also fixed flush with the inner surface of the cell wall vertically and horizontally to measure the local cell

wall coefficients (Fig. 1). Two blades of same length and width are attached to a hub at  $180^\circ$  by brazing. A brass shaft rod of 10 mm diameter is threaded in to the hub. The blades are at right angle to the shaft rod. This constitutes the 2-blade flat turbine (T). The shaft rod of the turbine is connected to the motor (SR) to rotate the turbine and is firmly kept in the cell in the centre of the cell walls and electrode support.

The electrolyte containing 0.01 N potassium ferricyanide and 0.01 N potassium ferrocyanide and 0.5 N NaOH is prepared in the cell. The turbine is rotated in the stagnant electrolyte at the desired speed. The limiting current data are obtained at all microelectrodes on the electrode support and cell wall. The limiting current represents the maximum rate of ion discharge. When potential is applied across the microelectrode and copper anode, negligible change in current for considerable increase in voltage indicates the limiting current. The electrochemical reaction occurring at the surface of the electrode is -



The limiting current data are measured for different heights of the turbine from the cell bottom to identify the optimum turbine height for mass transfer coefficient. From the experimental observations, the optimum turbine height from the cell bottom is 0.095 m. At this optimum height, the experiments are repeated varying the rotational speed, turbine diameter and blade width. 120 L of electrolyte is prepared in the storage tank and circulated through the cell. The effects of N, d and w are investigated for different electrolyte flow rates. The mass transfer coefficient is calculated from the relation:  $k_L = I/(nAFC_i)$ . The range of variables investigated are compiled in Table 1.

**Table 1: Range of variables investigated**

| Variable                                                    | Minimum | Maximum   |
|-------------------------------------------------------------|---------|-----------|
| Volumetric flow rate, $Q \times 10^5, \text{ m}^3/\text{s}$ | 3.39    | 56.94     |
| Diameter of the turbine, d, m                               | 0.05    | 0.09      |
| Length of the turbine blade, L, m                           | 0.02    | 0.04      |
| Width of the turbine blade, w, m                            | 0.005   | 0.015     |
| Rotational speed, N, rpm                                    | 250     | 2,000     |
| Reynolds number, $Re_f$                                     | 168     | 3,157     |
| Rotational Reynolds number, $Re_r$                          | 35,335  | 7, 04,733 |

## RESULTS AND DISCUSSION

The enhancement of mass transfer coefficient depends on the flow patterns generated by the turbine in the cell. The flow pattern depends on radial, longitudinal and tangential (rotational) components. As a vertical shaft is used in this investigation, the radial and tangential components act in a horizontal plane and provide the mixing action where as the tangential component acts in a vertical plane. When the turbine is rotating, the electrolyte moves to the cell bottom, spreads radially in all directions, flows upward along the walls and electrode support and returns to the electrolyte surface along the walls and sucked to the turbine. Another circulatory pattern flows upward towards the surface and back to the turbine. The increased flow rate of the electrolyte also increases the mass transfer coefficient.

The average mass transfer coefficient ( $k_{L,av}$ ) is obtained by calculating the simple arithmetic average of local mass transfer coefficients on electrode support or cell wall.  $k_{L,av}$  is drawn against turbine height from the cell bottom in Fig. 3. The  $k_{L,av}$  is slightly higher at a turbine height of 0.095 m than  $k_{L,av}$  values at other heights of the turbine from cell bottom. Hence, the other mass transfer data are obtained at this turbine height. The  $k_L$  values averaged row wise are drawn against electrode height from cell bottom (Fig. not shown). The mass transfer coefficient is slightly higher at an electrode height equal to the turbine height (0.095 m) than the values at other electrode heights from cell bottom. The effect of electrode distance from the cell wall on mass transfer coefficient is marginal.

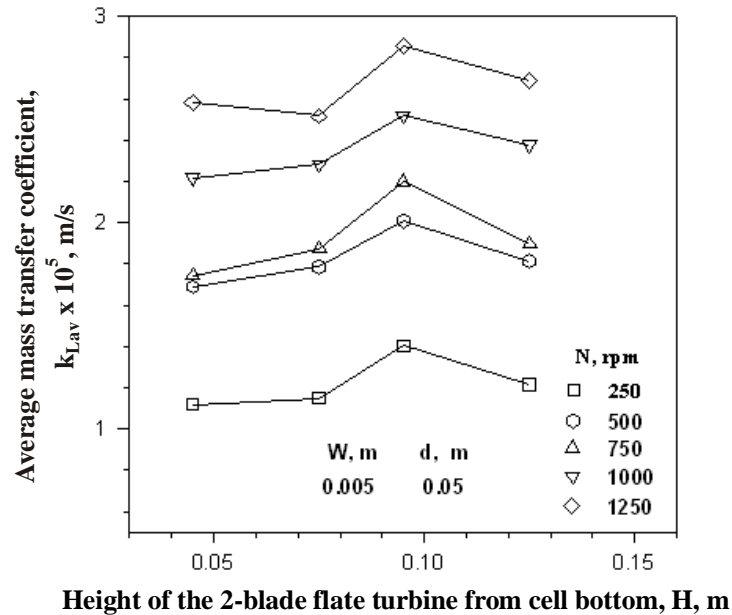


Fig. 3: Effect of turbine height from the cell bottom on average mass transfer coefficient

### Effect of rotation on mass transfer coefficient in stagnant electrolyte

#### Data on electrode support

The average mass transfer coefficient is increased with an increase in the rotational speed of the turbine (Fig. not shown) and is proportional to  $N^{0.38}$ . Also,  $k_{L,av}$  increases with an increase in 'd'. These observations are similar to these reported earlier<sup>1,2</sup>. The  $k_{L,av}$  is drawn against  $v_r$  for different 'd' and 'w' values in Figs. 4 and 5. The plots in Fig. 4 indicate the additional effect of 'd' on  $k_{L,av}$ . The  $k_{L,av}$  increases with increase in width of the turbine blade and  $k_{L,av}$  is proportional to  $w^{0.13}$  as per Fig. 5. The augmentation of mass transfer coefficient due to rotation is expressed as  $(k_{L,av}/k_{L,0})-1$ . The analysis of the data indicates 3.7 to 17 fold enhancement in mass transfer coefficient due to rotation of the turbines having dimensions of  $w = 0.005$  m,  $d = 0.05$  m,  $N = 250$  rpm and  $w = 0.015$  m,  $d = 0.09$  m,  $N = 1250$  rpm. The higher coefficients are due to the turbulence generated by the turbine and the overall flow pattern in the cell section as the turbine induces axial flow along with radial and swirl flows. The data are presented in terms of  $Sh_r/Sc^{1/3}$  and  $Re_r$  to account for changes in physical properties of the electrolyte. These data are correlated by the following equation using regression analysis.

$$Sh_r/Sc^{1/3} = 14.3 Re_r^{0.38} (w/d_e)^{0.13} \quad \dots(1)$$

The average deviation is 2.7 percent and the standard deviation is 3.5 percent.

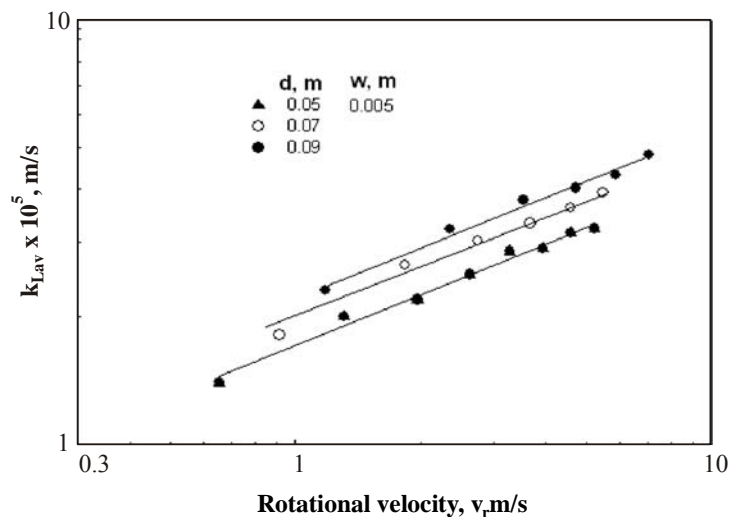


**Fig. 4: Dependence of average mass transfer coefficient on rotational velocity with turbine diameter as a parameter**

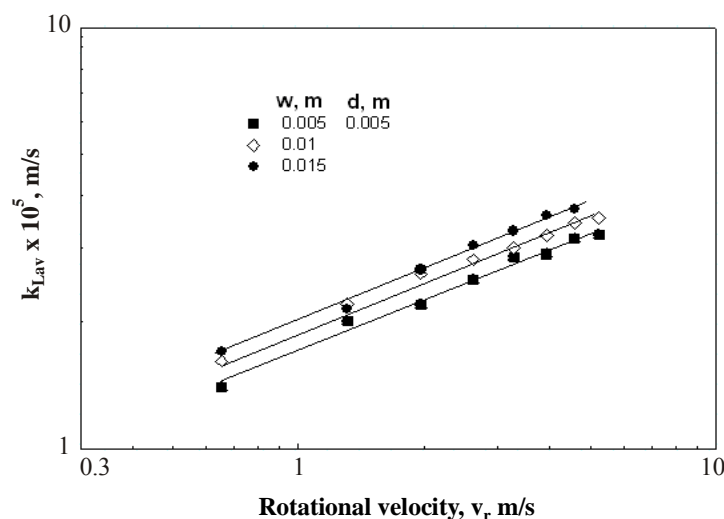


**Fig. 5: Dependence of average mass transfer coefficient on rotational velocity with blade width as a parameter**

### Data on cell wall

The mass transfer data obtained on cell wall are also analyzed in the above lines. The  $k_{L,av}$  increases with increases in  $v_r$ ,  $d$  and  $w$ . The mass transfer coefficients on the cell wall are enhanced from 3.3 to 16.7 fold due to the rotation over the value in stagnant electrolyte. The following equation is found to be the best fit for the mass transfer data obtained on cell wall.

$$Sh_r/Sc^{1/3} = 1.7 Re_r^{0.4} (w/d_e)^{0.14} \quad \dots(2)$$

Average deviation is 2.9% and standard deviation is 3.8%. Fig. 6 compares the present data obtained on the electrode support (line A) with the data obtained on cell wall (line B). The magnitude of mass transfer coefficient on electrode support and cell wall are more or less same. The mass transfer data of Sedahmed et al.,<sup>1</sup> obtained in a cylindrical agitated vessel are shown in the same fig. as line C for comparison. The plots indicate 130 to 180% enhancement in mass transfer coefficient in the closed vessel than the present data in

the Reynolds number range of 35, 335 and 1, 05, 280. The reason can be attributed to the open cell used in the present investigation in stead of closed vessel used by Sedahmad et al., The open cell alters the hydrodynamics in the cell and the turbulence generated by the turbine will be generally lessened.

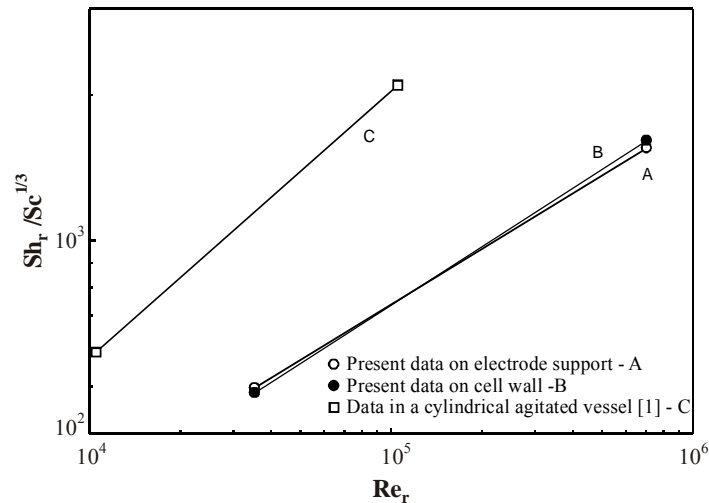


Fig. 6: Comparison of present data for rotation of turbine with that of Sedahmed [1]

### Effect of rotation on mass transfer coefficient in flowing electrolyte

#### Data on electrode support

It is evident from Fig. 7 that increased electrolyte velocity results in higher mass transfer coefficient. It is also noted that  $k_{L,av}$  increases with increase in 'd'. The plots drawn in Figs. 8 and 9 between  $k_{L,av}$  and  $v_r$  indicate that the average mass transfer coefficient increases with an increase in  $v_r$  and is proportional to  $v_r^{0.12}$ .  $k_{L,av}$  is further increased with increase in 'd'. Also  $k_{L,av}$  increases with increased 'w'. The maximum mass transfer coefficients are obtained for a rotating turbine of  $d = 0.09$  m,  $w = 0.015$  m and  $N = 750$  rpm.

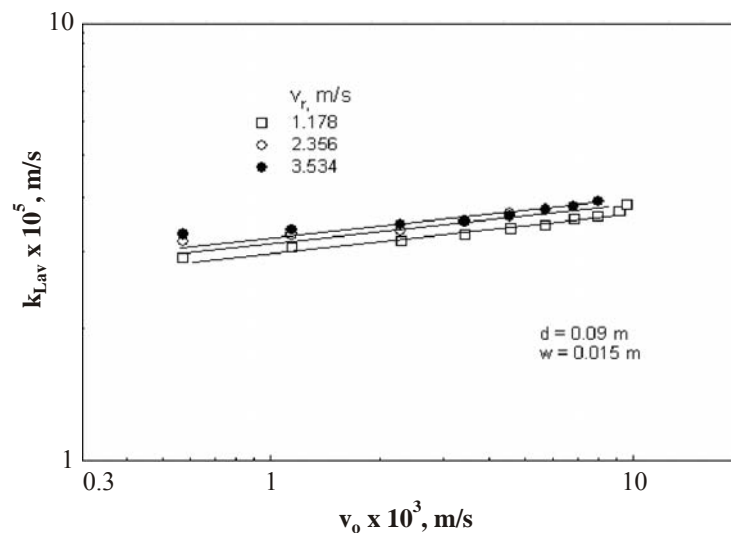
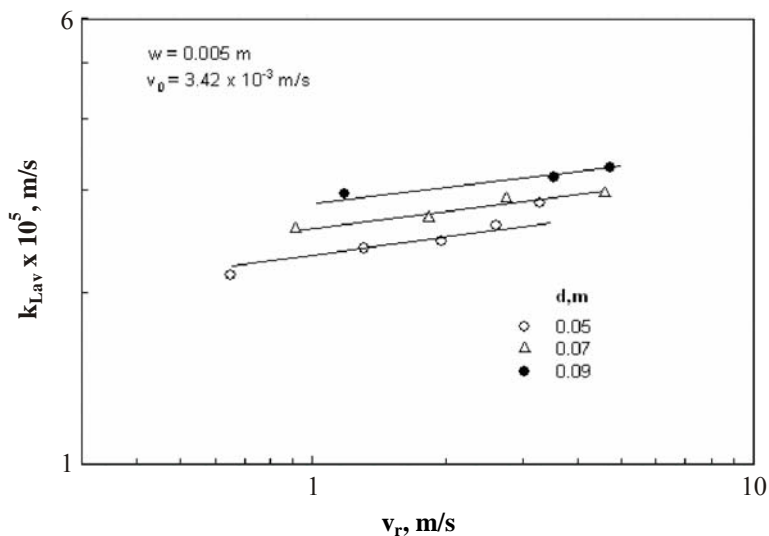
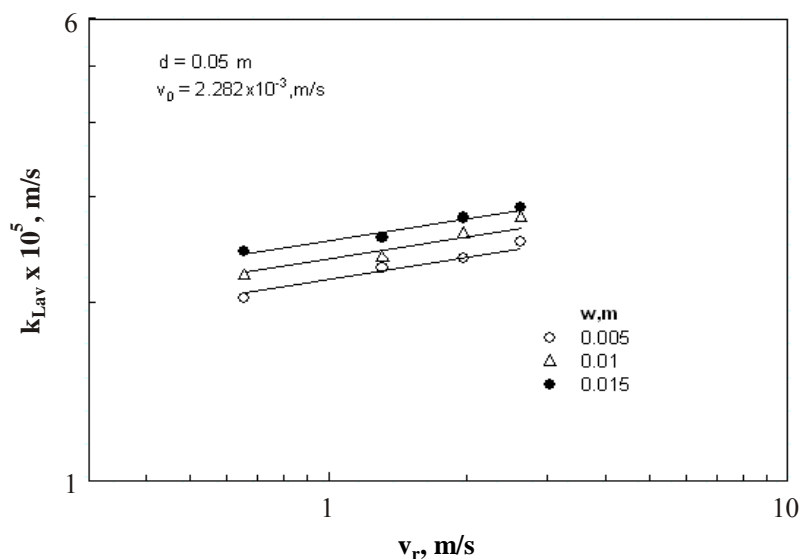


Fig. 7: Average mass transfer coefficient versus electrolyte velocity –Effect of rotational velocity.



**Fig. 8: Average mass transfer coefficient as a function of rotational velocity – Effect of turbine diameter**



**Fig. 9: Dependence of average mass transfer coefficient on rotational velocity- Effect of blade width**

The minimum coefficients are obtained for the rotating turbine of  $d = 0.05$  m,  $w = 0.005$  m and  $N = 250$  rpm. The augmentation of mass transfer coefficient in this investigation due to rotation and forced convection flow is 5.7 to 12.7 fold over the value in stagnant electrolyte. However, the augmentation is 1.33 to 4 fold over the value for forced convection flow. It is evident that the higher mass transfer coefficient is due to the turbulence generated by the impeller and higher velocity of the electrolyte in the cell. Based on the effects of  $v_r$ ,  $d$ ,  $w$  and  $v_0$  on  $k_{Lav}$ , the present data are correlated by the following equation using regression analysis.

$$Sh_r/Sc^{(1/3)} = 190 Re_r^{0.12} Re_f^{0.1} (w/d_e)^{0.125} \quad \dots(3)$$

The average deviation is 4.47% and the standard deviation is 7.35%.

### Data on cell wall

The mass transfer data obtained on cell wall for rotation of the turbine and forced convection flow of the electrolyte are analyzed in the lines described above. The  $k_{L,av}$  is found to increase with increases in  $v_r$ ,  $d$ ,  $w$  and  $v_o$ . The augmentation in mass transfer coefficient on the cell wall is 1.25 to 4 fold over the value for forced convection flow. The augmentation is 5.2 to 11 times due to rotation and forced convection flow of the electrolyte. The mass transfer coefficients obtained are approximately equal on electrode support and cell wall. The data on cell wall are correlated by the following equation with an average deviation of 4.57% and standard deviation of 8%.

$$Sh_r/Sc^{1/3} = 280 Re_r^{0.1} Re_f^{0.1} (w/d_e)^{0.1} (d/d_e)^{0.17} \quad \dots(4)$$

The present data obtained on electrode support for rotation of the turbine in forced convection flow of the electrolyte (line D) are compared in Fig. 10 with the data obtained without any electrolyte flow (line A). The mass transfer data with forced convection flow (line D) are twice the data without electrolyte flow at low Reynolds number (33,500). The mass transfer coefficient with electrolyte flow gradually approaches the mass transfer coefficient value for rotation of the turbine without forced convection flow at  $Re_r = 5,00,000$ . This observation indicates that the electrolyte flow rate does not influence the mass transfer coefficient for Reynolds number  $> 5,00,000$ .

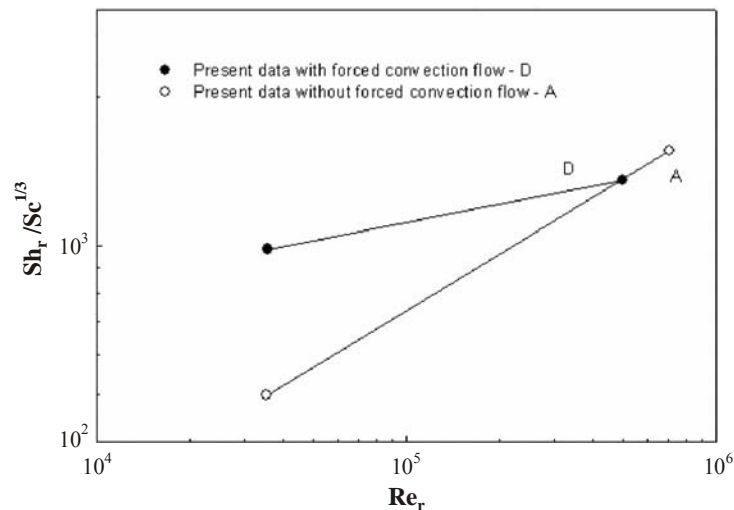


**Fig. 10: Mass transfer data on electrode support for rotation of turbine with and without forced convection flow**

### CONCLUSION

The maximum mass transfer coefficient is obtained when the turbine is rotated at a height of 0.095 m from cell bottom. The mass transfer coefficient increases with an increase in electrode height from the cell bottom up to 0.095 m and decreases beyond that height. The effect of electrode distance from the cell wall is marginal on mass transfer coefficient. The mass transfer rate is increased with increases in rotational velocity and electrolyte velocity. The mass transfer rate is increased with the increased width of the turbine blade and turbine diameter. The enhancement in mass transfer coefficient on the electrode support due to rotation of the turbine is 3.7 to 17 fold where as the power requirement is increased from 10 to 60 watts in the range of variables studied. The mass transfer enhancement due to rotation and forced convection flow of the electrolyte is 5.7-12.7 fold for the turbine having dimensions of  $d = 0.05$  m,  $w = 0.005$  m and  $N = 250$  rpm and for the turbine having dimensions of  $d = 0.09$  m,  $w = 0.015$  m and  $N = 750$  rpm over the value in

stagnant electrolyte. Similar observations are noted for the mass transfer data obtained on cell wall. The data are augmented by 3.3 to 16.7 fold due to rotation and 5.2 to 11 fold due to combined rotation and forced convection flow over the value in stagnant electrolyte in the range of variables investigated.

### Nomenclature

|            |                                                                              |
|------------|------------------------------------------------------------------------------|
| A          | Area of the microelectrode, $m^2$                                            |
| $C_i$      | Concentration of the ferricyanide ion, $k \text{ mole}/m^3$                  |
| d          | diameter of the 2-blade flat turbine/ sphere/ cylinder/ impeller, m          |
| $d_h$      | Hydraulic diameter, m                                                        |
| $d_o$      | Diameter of the outer electrode, m                                           |
| $d_e$      | Equivalent diameter of the electrolytic cell, $4Wh/(2h + W)$ , m             |
| $D_L$      | Diffusivity of ferricyanide ion, $m^2/s$                                     |
| F          | Faraday's constant, coulombs/gm equivalent                                   |
| h          | Height of the electrolyte in the cell, m                                     |
| $h_g$      | Gap between cylindrical electrode and cell wall, m                           |
| H          | Distance between the wires, m                                                |
| $H_n$      | Distance of the nozzle from the target surface, m                            |
| I          | Limiting current, A                                                          |
| L          | Length of the turbine blade, m                                               |
| $k_L$      | Local mass transfer coefficient, $I/(nAFC_i)$ , m/s                          |
| $k_{L,av}$ | Average mass transfer coefficient for 2-blade flat turbine, m/s              |
| $k_{L,o}$  | Mass transfer coefficient in stagnant electrolyte, m/s                       |
| $k_{L,v}$  | Mass transfer coefficient for vibration of cone/ disc/ sphere/ impeller, m/s |
| $k_{L,r}$  | Mass transfer coefficient for rotation of cone/ disc/ sphere, m/s            |
| $k_{L,vr}$ | Mass transfer coefficient for vibration and rotation, m/s                    |
| N          | Rotational speed of the 2-blade flat turbine/ impeller, rpm                  |
| n          | Number of electrons transferred in the reaction                              |
| Q          | Volumetric flow rate of the electrolyte, $m^3/s$                             |
| r          | Cylinder radius, m                                                           |
| $\bar{r}$  | Cylinder mean radius, m                                                      |
| $r_2$      | External radius, m                                                           |
| $v_o$      | Electrolyte velocity, $4Q/(\pi d_e^2)$ , m/s                                 |
| $v_r$      | Rotational velocity, $\pi dN/60$ , m/s                                       |
| $v_v$      | Vibrational velocity, m/s                                                    |
| W          | Width of the electrolytic cell, m                                            |

|                   |                                                                           |
|-------------------|---------------------------------------------------------------------------|
| W                 | Width of the turbine blade, m                                             |
| Sh                | Sherwood number, $kd_h/D_L$                                               |
| Sh <sub>r</sub>   | Sherwood number, $k_{L,av} d_e/D_L$                                       |
| Sh <sub>v,r</sub> | Sherwood number for simultaneous vibration and rotation, $k_{L,vr} d/D_L$ |
| Sh <sub>v</sub>   | Sherwood number for vibration, $k_{L,v} d/D_L$                            |
| Sh <sub>L</sub>   | Sherwood number for rotation, $k_{L,r} d/D_L$                             |
| Sh <sub>c</sub>   | Sherwood number, $k_{L,r} d_o/D_L$                                        |
| Sh <sub>d</sub>   | Sherwood number, $k_{L,r} d_h/D_L$                                        |
| Sc                | Schmidt number, $\mu/(\rho D_L)$                                          |
| Re                | Reynolds number, $\rho N d^2/(60 \mu)$                                    |
| Re <sub>1</sub>   | Reynolds number, $\omega r^2/\nu$                                         |
| Re <sub>c</sub>   | Reynolds number, $\rho N d h_g/(60 \mu)$                                  |
| Re <sub>d</sub>   | Reynolds number, $\rho N r_2 d_h/(60 \mu)$                                |
| Re <sub>v</sub>   | Vibrational Reynolds number, $\rho d v_v/\mu$                             |
| Re <sub>r</sub>   | Rotational Reynolds number, $\rho d v_r/\mu$                              |
| Re <sub>f</sub>   | Reynolds number, $\rho d_e v_o/\mu$                                       |
| J <sub>D</sub>    | Mass transfer factor, $(k_{L,av}/v_o) Sc^{2/3}$                           |
| J <sub>Dr</sub>   | Mass transfer factor, $(k_{L,r}/v_r) Sc^{2/3}$                            |
| $\rho$            | Density of the electrolyte, $kg/m^3$                                      |
| $\mu$             | Viscosity of the electrolyte, $kg/(ms)$                                   |
| $\omega$          | Angular velocity, $rad/s$                                                 |
| $\alpha$          | Cone apex half angle, $deg$                                               |
| $\nu$             | Kinematic viscosity, $m^2/s$                                              |

## REFERENCES

1. G. H. Sedahmed, H. A. Farag, A. M. Kayar and I. M. El-Nashar, Mass Transfer at the Impellers of Agitated Vessels in Relation to their Flow- Induced Corrosion, *Chem. Engg. J.*, **71**, 57-65 (1998).
2. Z. D. Chen and J. J. J. Chen, Comparison of Mass Transfer Performance for Various Single and Twin Impellers, *Int. J. Heat and Mass Transfer*, **77**, 104-109 (1999).
3. Wei-Ming Lu, Hong-Zhang Wu and Cheng-Ying Chou, Effect of Impeller Blade Number on  $K_L a$  in Mechanically Agitated Vessels *Korean J. Chem. Engg.*, **16(5)**, 703-708 (1999).
4. Thomas Moucha, Vaclav Linek and Eva Prokopova, Gas Hold-up, Mixing Time and Gas-Liquid Volumetric Mass Transfer Coefficient of Various Multiple-Impeller Configurations: Rushton Turbine, Pitched Blade and Techmix Impeller and their Combinations, *Chemical Engineering Science*, **58**, 1839-1846 (2003).
5. M. S. Krishna and G. J. V. J. Raju, Ionic Mass Transfer in Agitated Vessels Part I- Studies on Design Variables of Stirred Tank, *Indian J. Technol.*, **3**, 263-267 (1965).

6. B. Bharati, P. Venkateswarlu, S. Kiran Appaji, B. Sanyasi Rao and G. J. V. Raju, Ionic Mass Transfer for Vibrating and Rotating Spheres, *Chemical Engineering and Processing*, **36**, 59-65 (1997).
7. F. Coeuret and J. Legrand, Mass and Momentum Transfer at the Rotating Surface of a Continuous Annular Electrochemical Reactor, *Electrochimica Acta*, **28**, 611-617 (1983).
8. F. S. Afshar, D. R. Gabe and B. Sewell, Mass Transfer at Rotating Cone Electrodes, *J. Appl. Electrochem.*, **21**, 32-39 (1991).
9. P. King, V. S. R. K. Prasad and G. Hanumantha Rao, Studies on Ionic Mass Transfer at Central Electrode in the Impingement Region on a Rotating Disc with a Submerged Impinging Jet in a Closed Cell, *Indian Chem. Engr.*, **46**, 244-250 (2004).
10. V. Subramanian, M. S. Krishna and P. Adivarahan, Mass Transfer Studies with Symmetrically Rotating Bodies, *Indian J. Technol.*, **4**, 353-358 (1966).
11. C. I. Elsner, P. L. Schilardi and S. L. Marchiano, A Phenomenological Approach to Ionic Mass Transfer at Rotating Disc Electrodes with a Hanging Column of Electrolyte Solution, *J. Appl. Electrochem.*, **23**, 1181-1186 (1993).
12. Aldona Jagminiene, Ina Stankeviciene and Algirdas Vaskelis, Autocatalytic Copper (II) Reduction by Cobalt (II) – Ethylenediamine Complex Studied by Rotating Disc Electrode Technique, *Chemija(Vilnius)*, **14(3)**, 140-144 (2003).
13. D. R. Gabe and P. A. Mankajuola, Enhanced Mass Transfer Using Roughened Rotating Cylinder Electrodes in Turbulent Flow, *J. Appl. Electrochem.*, **17**, 370-384 (1987).
14. N. A. Pokryvailo, E. B. Kaberdina and M. I. Syrkin, Unsteady Mass Transfer in Turbulent Flow Close to a Rotating Cylinder, *J. Appl. Electro Chemistry*, **21**, 1077-1080 (1991).
15. B. Morrison, K. Striebel, P. N. Ross, Kinetic Studies Using a Rotating Cylinder Electrode Part 1: Electron Transfer Rates in Ferrous/Ferric Sulfate on Platinum, *J. Electro-Analytical Chem.*, **215**, 151-160 (1986).
16. J. M. Grau and J. M. Bisang, Mass Transfer Studies at Packed Bed Rotating Cylinder Electrodes of Woven-Wire Meshes, *J. Appl. Electrochem.*, **36**, 759-763 (2006).